Postharvest Biology and Technology 212 (2024) 112889

Contents lists available at ScienceDirect

Postharvest Biology and Technology

journal homepage: www.elsevier.com/locate/postharvbio

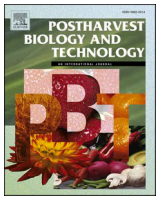

Transcriptomic and volatilomic profiles reveal *Neofabraea vagabunda* infection-induced changes in susceptible and resistant apples during storage

Paolo Baldi [a], Matteo Buti [b,*], Valeria Gualandri [c], Iuliia Khomenko [a], Brian Farneti [a], Franco Biasioli [a], Donatella Paffetti [b], Mickael Malnoy [a]

[a] Research and Innovation Centre, Fondazione Edmund Mach, San Michele all'Adige, Trento 38010, Italy
[b] Department of Agriculture, Food, Environmental and Forestry Sciences (DAGRI), University of Florence, Florence 50144, Italy
[c] Technology Transfer Centre, Fondazione Edmund Mach, San Michele all'Adige, Trento 38010, Italy

ARTICLE INFO

Keywords:
Apple pathogen
Postharvest disease
Neofabraea vagabunda
Bull's eye rot
Transcriptomics
VOCs

ABSTRACT

Bull's eye rot is one of the most severe diseases that may affect apple fruit during post-harvest storage. It is caused by the fungus *Neofabraea vagabunda*, and the mechanism by which the pathogen infects the fruits is only partially understood. In particular, very little is known about the molecular mechanisms regulating the interaction between the pathogen and the host during symptoms development. Despite different apple cultivars show divergent levels of resistance to the pathogen, the genetic basis of these responses is still unknown. In order to better understand the molecular mechanisms occurring in the apple fruit during *N. vagabunda* infection, a large-scale transcriptome study by RNA-Seq analysis was performed, comparing fruits of the sensitive 'Roho' cultivar and the resistant cultivar 'Ariane' after artificial infection with *N. vagabunda* and a storage period of four months. Transcriptomic analyses revealed the regulation of several classes of genes during this period, some of which may be involved in apple-pathogen interaction, such as superoxide dismutases and heat shock proteins (HSPs), ethylene-responsive transcription factors (ERFs), carboxylesterases and NAC transcription factors gene families. Moreover, a volatile analysis was performed, revealing differences in the volatile profile between the resistant and the susceptible cultivar that may help to elucidate the resistance mechanism. RNA-Seq data highlighted several classes of pathogen-related genes, such as genes coding for enzymes involved in cell wall disruption and in reactive oxygen species (ROS) homeostasis, being differentially regulated between resistant and susceptible fruits and between diseased and healthy fruits of the same cultivar, indicating that apples are capable of perceiving and triggering a molecular response to *N. vagabunda* infection. Some volatiles, as ethanol and methanol, but also furan and formaldehyde, might be potential markers for *N. vagabunda* infection; others, such as hexenal and methyl acetate, were found to be putatively involved in regulating apple-fungi interaction.

1. Introduction

Apple (*Malus* x *domestica* Borkh.) is one of the most economically important fruit crops in the world. Beside their organoleptic and healthy properties, apples are also appreciated for the possibility to be conserved for months at low temperature remaining crisp. Nevertheless, several problems can occur during apple storage, going from physiological disorders to different types of rot (Buti et al., 2018; Nybom et al., 2020). Some of the most important apple storage rots belong to necrotrophic genus of *Neofabraea*; in particular, *N. vagabunda* (syn. *N. alba; Phlyctema vagabunda*) is the agent of bull's eye rot (BER), a disease that can severely decrease fruit quality and marketability, causing serious economic losses, especially in highly susceptible cultivars such as 'Roho' (Cameldi et al., 2017). *N. vagabunda* can infect apples in the orchard at different developmental stages, with ripening being the stage at which the fruit is most susceptible. Conidia formation and dispersion is favored by high humidity and cool temperatures (Köhl et al., 2018). After infection, the symptoms are not immediately evident, as the pathogen can remain quiescent for several months. During apple storage, when growing conditions are optimal, the fungus starts to develop causing fruit decay. The mechanism by which *N. vagabunda* breaks the dormancy is still unknown, even though it is probably due to fruit physiological changes associated to a certain stage of maturity or to a decline of fruit antifungal compounds and defense responses (Cameldi et al., 2017). For

* Corresponding author.
E-mail address: matteo.buti@unifi.it (M. Buti).

https://doi.org/10.1016/j.postharvbio.2024.112889
Received 15 November 2023; Received in revised form 5 March 2024; Accepted 7 March 2024
Available online 12 March 2024

biotrophic fungi, infection ability can be deeply influenced by the host response due to the activation of sophisticated recognition and signaling networks. As a result of fungal attacks, plants can accumulate reactive oxygen species (ROS) and activate various defense pathways (Janisiewicz et al., 2016). Ascorbate and glutathione content can also increase as the plant needs to remove the excess of ROS (Nybom et al., 2020). Ethylene- and jasmonic acid-related pathways are hypothesized to play a major role in modifying apple resistance to rot, together with the phenylpropanoid metabolism (Lv et al., 2018). Another factor that can influence fruit susceptibility to various types of rot is the pectin degradation of the cell wall during ripening (Di Francesco et al., 2019). Other studies pointed out modifications in total phenols, sugar content and antioxidants (Bui et al., 2019).

During the whole storage period, apples produce many volatile organic compounds (VOCs). In a recent study, it was observed that the volatile profile may change during the ripening process, apparently influencing BER development, and that, during the infection process, pathogens could also produce VOCs, some of which may play a role in the interaction with the host (Neri et al., 2019). Despite few information is available on apple VOCs production during *N. vagabunda* infection, in the same study it was observed that methanol and ethanol are the earliest markers of BER, and that VOCs related to senescence are probably involved in stimulating pathogen hyphal growth.

Nowadays, sensitive and non-invasive techniques are available for the detection of VOCs, such as proton transfer reaction-time of flight-mass spectrometry (PTR-ToF-MS). In the present work, we combined RNA-Seq technology with PTR-ToF-MS analysis to study gene expression changes during storage and VOCs production of two apple cultivars, one susceptible ('Roho') and one resistant ('Ariane') to BER. Gene expression and VOCs production were estimated and compared at the beginning of the storage period and after 4 months of storage in order to detect: (i) genes that are regulated during the storage period and may influence pathogen-host interaction; (ii) genes that are differentially regulated in healthy and diseased apples; (iii) genes that are differentially regulated between the resistant and susceptible cultivar; (iv) differences in the volatile profile between the resistant and the susceptible cultivar that may help to elucidate the resistance mechanism. To our knowledge, this is the first transcriptomic study on apple during *N. vagabunda* infection, and may contribute to better understand the mechanism of BER development and host-pathogen interaction.

2. Materials and methods

2.1. Plant material, N. vagabunda inoculation and storage conditions

Apple fruits of the cultivars 'Ariane' and 'Roho' were harvested at commercial ripening stage from an orchard belonging to the Edmund Mach Foundation, located in Trentino region in northern Italy (latitude 46.179766°, longitude 11.117726°). The harvested apples maturity was assessed according to the following maturity indexes: flesh firmness of 7–8 kg cm^{-2}, clearings extending to 50–60% of the fruit cortex through a starch iodine test (Smith et al., 1979). After harvest, thirty fruits for each cultivar were artificially inoculated by spraying an inoculum of *N. vagabunda*. For inoculum preparation, the isolate CBS102871 of *N. vagabunda* was grown in tomato agar and incubated in the dark at 15 °C (Cameldi et al., 2017). After 21 days, conidial suspension was prepared by scraping mycelium, suspending it in sterile deionized water and adjusting to the final concentration (10^5 conidia mL^{-1}). Immediately after the inoculation, the peels of three randomly selected fruits for 'Ariane' (AC) and 'Roho' (RC) cultivars were sampled for RNA extraction and immediately frozen in liquid nitrogen, while the remaining fruits were stored at 4 °C with a relative humidity of 95% for four months. After the cold storage, the peels of three randomly selected 'Ariane' inoculated fruits not showing bull's eye rot symptoms (AI), three randomly selected 'Roho' inoculated fruits not showing bull's eye rot symptoms (RI) and three randomly selected 'Roho' inoculated fruits showing bull's eye rot symptoms (RD) were sampled for RNA extraction and immediately frozen in liquid nitrogen. The expected biological variability in our study was very low due to the controlled conditions so, according to the vast majority of published studies with the same characteristics, three biological replicates were carried out for RNA-Seq experiment (Li et al., 2022; Negussu et al., 2023).

Moreover, five apples for each cultivar and condition (AC; RC; AI; RI and RD) were randomly selected and used for VOCs analysis using PTR-ToF-MS. According to previously published studies with similar experimental designs, five biological replicates were considered sufficient for a robust VOCs analyses (Farneti et al., 2015, 2022).

2.2. RNA isolation and sequencing

Total RNA was extracted from apple peel samples using the Spectrum plant total RNA kit (Sigma-Aldrich, St. Louis, MO, USA), according to the manufacturer's instructions, including the on-column DNase digestion step. In order to assess the integrity of the genetic material, 1 μL of each RNA was loaded onto 1.5% agarose gel and visualized using ChemiDoc XRS gel imaging system (Bio-Rad, Hercules, CA, USA). RNA samples were then quantified using Nanodrop 8000 spectrophotometer (Thermo Fisher Scientific, Waltham, MA, USA). Synthesis of the cDNAs used for reverse transcription quantitative PCR (RT-qPCR) reactions was performed with Superscript III reverse transcriptase (Thermo Fisher Scientific, Waltham, MA, USA) using 5 μg of total RNA and 1 μL of oligo (dT)20 (50 μM) as a primer. RNA libraries were prepared with NEBNext® Ultra™ RNA Library Prep Kit (New England BioLab) and sequenced using an Illumina NovaSeq6000 system at Novogene (Cambridge, UK), generating 150- base pair paired-end reads.

2.3. RNA-Seq data validation by RT-qPCR

Expression levels of 10 selected genes were tested by reverse transcription quantitative PCR (RT-qPCR), using ViiA 7 real-time PCR system (Life Technologies, Carlsbad, CA, USA). Platinum SYBR Green qPCR SuperMix-UDG (Life Technologies, Carlsbad, CA, USA) was used as fluorescent dye. Primers were designed using the online software Primer3Plus (https://www.bioinformatics.nl/cgi-bin/primer3plus/primer3plus.cgi). The reverse transcription qPCR reactions were carried out using 1 μl of diluted (1:10) cDNA and the following reaction conditions: 2 min at 50 °C, 2 min at 95 °C followed by 40 cycles at 95 °C for 15 s and 60 °C for 30 s. A control sample without the template was included for each primer combination, and a melt-curve analysis was performed at the end of each reaction in order to exclude unspecific amplification. All experiments were carried out using three independent biological replicates. Ct values were calculated by the ViiA 7 software based on the Ct values obtained from three technical replicates per sample. *Actin* was used as housekeeping gene. Expression profiles were obtained using the comparative Ct method (Pfaffl, 2001).

2.4. Volatile analysis

Fruits were analyzed non-invasively by a commercial PTR-ToF-MS 8000 apparatus (Ionicon Analytik GmbH, Innsbruck, Austria) at the beginning of the storage period and after four months of storage. VOCs measurements were performed in five replicates, for each cultivar and treatment, where a single apple was put inside 1.3 L glass jar and left closed for 30 min at room temperature (21±1 °C) for headspace incubation. VOCs were then measured by direct injection of the head space mixture into the PTR-ToF-MS drift tube, set with the following conditions: 110 °C drift tube temperature, 2.8 mbar drift pressure, 628 V drift voltage in active RF mode. This leads to an E/N ratio of about 130 Townsend (Td; 1 Td = 10^{-17} Vcm^2), where E corresponds to the electric field strength and N to the gas number density. The sampling time per channel of ToF acquisition was 0.1 ns, amounting to 350,000 channels for a mass spectrum ranging up to $m/z = 400$. Every single spectrum is

the sum of about 28.600 acquisitions lasting 35 μs each, resulting in a time resolution of 1 s. Sampling measurement was performed in 60 cycles resulting in an analysis time of 60 s/sample.

2.5. Data analysis

The good quality of the RNA-Seq raw reads was assessed with FastQC v0.11.5 (http://www.bioinformatics.babraham.ac.uk/projects/fastqc), while the removal of the adapters sequences and the low-quality reads

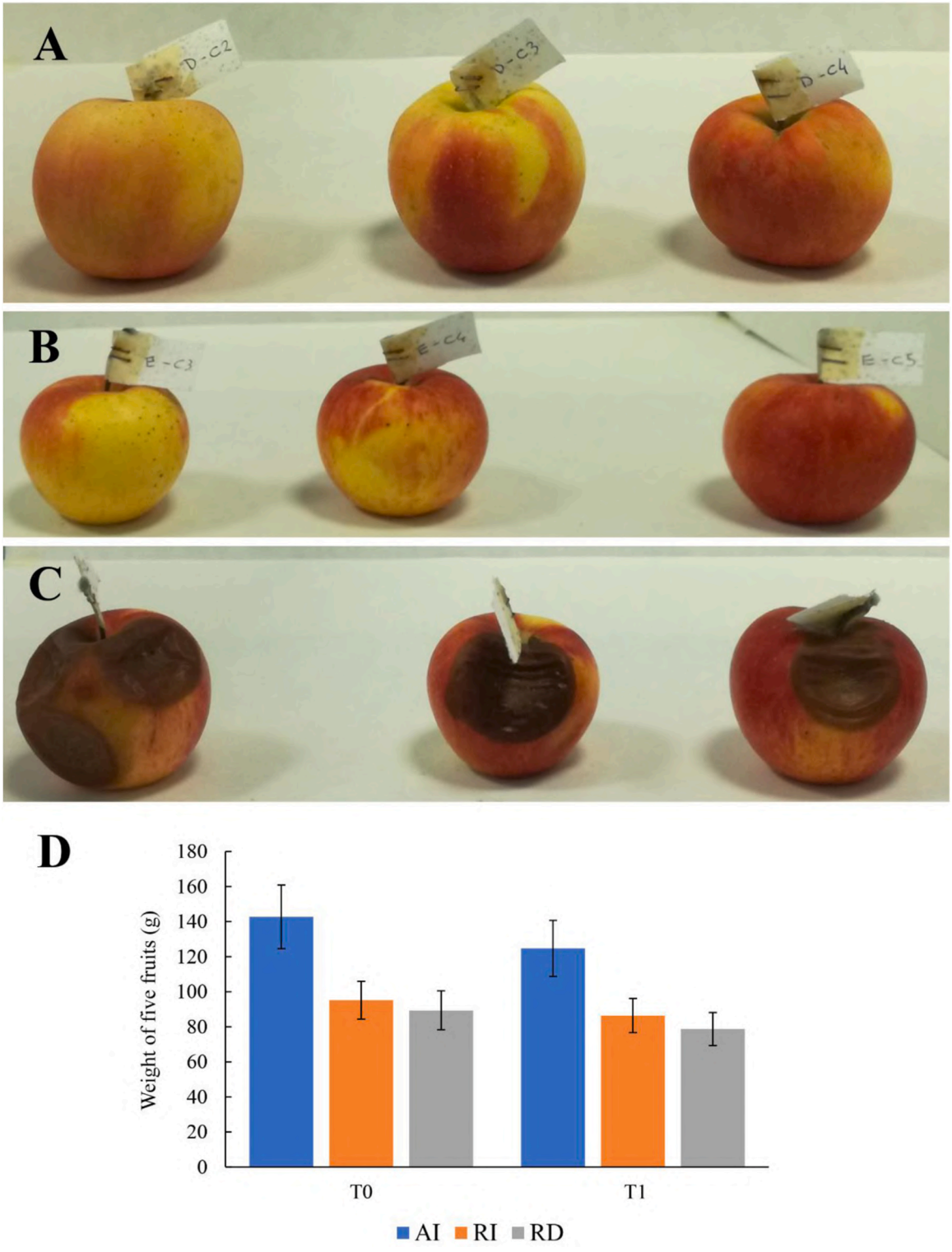

Fig. 1. A. Apple fruits of the resistant cultivar 'Ariane' after four months of storage. B. Apple fruits of the susceptible cultivar 'Roho' showing no symptoms of bull's eye rot after four months of storage. C. Apple fruits of the susceptible cultivar 'Roho' showing symptoms of bull's eye rot after four months of storage. D. Bar plot visualizing the weight in grams of five fruits of 'Ariane' apples without symptoms (AI), 'Roho' apples without symptoms (RI) and 'Roho' apples with symptoms (RD) at the beginning of the storage period (T0) and after four months of cold storage (T1); error bars were displayed.

were carried out using Trimmomatic v0.39 (Bolger et al., 2014) with the settings ILLUMINACLIP:adapters.fa:2:30:10 LEADING:3 TRAILING:3 SLIDINGWINDOW:4:15 MINLEN:36. The filtered reads of the 15 libraries were mapped to *Malus x domestica* GDDH13 v1.1 genome assembly (Daccord et al., 2017) using HiSat2 v2.2.1 (Kim et al., 2019). Reads counts were generated from the alignment files using featureCounts v1.6.0 software (Liao et al., 2014) with default parameters, basing on 'exon' feature and 'gene_id' meta-feature of GDDH13 v1.1 apple annotation file retrieved from the Genome Database for Rosaceae repository (https://www.rosaceae.org/).

Raw counts data elaborations and differential expression (DE) analyses were carried out using Bioconductor EdgeR v3.40.2 package (Robinson et al., 2009). In particular, EdgeR was used to filter out the not active genes (a gene was considered 'active' if reads per million mapping to that gene was >1 in at least two out of the fifteen libraries), normalize the RNA libraries, and visualize the multi-dimensional scaling (MDS) plot for RNA libraries normalized counts. MDS was used for samples dimensionality reduction because of its ability to capture non-linear relationships in processed RNA-Seq counts, strengthening the robustness and interpretability of sample distance representation. Then, the differential expression analyses were carried out with the likelihood ratio test. The genes with a resulting false discovery rate (FDR) lower than 0.01 and $\log_2$ Fold Change (LFC) lower than −2 or higher than 2 were considered as differentially expressed. Heatmap and Venn diagram representations of differentially expressed genes (DEGs) were visualized using the heatmap.2 function in the gplots v3.1.3 R package (https://github.com/talgalili/gplots) and Venny 2.1.0 webtool (https://bioinfogp.cnb.csic.es/tools/venny/), respectively.

Homologies against protein databases and GO annotations of the *Malus x domestica* GDDH13v1.1 transcripts were retrieved from the Genome Database for Rosaceae repository. Cytoscape 3.9.1 (https://cytoscape.org) with the BiNGO 3.0.5 plugin was used for the GO enrichment analyses (Maere et al., 2005). GO categories with corrected p-value <0.05 were considered as enriched. KEGG enrichment analyses were carried out with KOBAS 3.0 gene-list enrichment module using *Malus domestica* species background, and the results were plotted with ggplot2 v3.4.3 R visualization package (Bu et al., 2021; Wickham, 2016).

Statistical analysis of the RT-qPCR results was performed by *t* test.

The array of masses detected with PTR-ToF-MS was reduced by applying noise and correlation coefficient thresholds. The first removed peaks were not significantly different from blank samples; the latter excluded peaks with over 99% correlation, which correspond for the most part to isotopes of monoisotopic masses (Farneti et al., 2017).

3. Results

3.1. Apple infection and storage

Apple fruits of the resistant cultivar 'Ariane' and the susceptible cultivar 'Roho' were artificially inoculated with an inoculum of *N. vagabunda*. Three fruits for each cultivar were randomly selected and their peels were sampled ('Control'). The remaining fruits were stored at 4 °C for four months. None of the 'Ariane' fruits developed symptoms of bull's eye rot (Fig. 1A), while 75% of the 'Roho' fruits showed clear symptoms of the disease (Figs. 1B and 1C). Three fruits for each cultivar not showing symptoms were randomly selected and their peels were sampled ('Inoculated'). Three 'Roho' fruits showing clear symptoms of bull's eye rot were randomly selected and their peels were sampled ('Diseased'). All the fruits were weighted before and after the storage period in order to evaluate the water loss. In all cases, the water loss after four months of storage was comprised between 10% and 12% (Fig. 1D).

3.2. RNA sequencing, validation and differential expression analyses

A total of 15 RNA libraries were prepared and sequenced with Illumina NovaSeq 6000 sequencing system. The libraries were obtained from 'Ariane' control fruits (AC); 'Ariane' fruits inoculated with *N. vagabunda* showing no symptoms (AI); 'Roho' control fruits (RC); 'Roho' fruits inoculated with *N. vagabunda* showing no symptoms (RI); diseased 'Roho' fruits (RD) (Table 1). Overall, 676,112,981 paired 150 bp-long reads were generated, ranging from 35 to 52 million across the fifteen libraries (Table 1). After assessing their quality, RNA-Seq raw reads have been deposited in the ArrayExpress database at EMBL-EBI (https://www.ebi.ac.uk/biostudies/arrayexpress) under the accession number E-MTAB-13465.

Adapters sequences and low-quality nucleotides were filtered out, resulting in 95–97% of 'surviving' reads (Table 1). For each RNA library, 90–93% of filtered reads pairs were aligned to the apple GDDH13 v1.1 reference assembly (Table 1), and the number of reads mapping to each predicted gene was estimated according to GDDH13 v1.1 gene models.

After the 'not active' genes were filtered out (27,406 out of the 46,558 predicted apple genes resulted as 'active'), normalization factors were calculated according to each library size, and normalized reads counts were used for downstream analyses. Multi-dimensional scaling (MDS) plot showed high reproducibility, as the biological replicates were all closely clustered and clearly separated from the other samples, except for RI and RD samples, which clustered noticeably close (Fig. S1).

Differential expression analyses for four pairwise comparisons were carried out: AI *vs.* AC; RI *vs.* RC; RD *vs.* RC; RC *vs.* AC. The first three comparisons determined the genes regulated after four months of storage, while the fourth comparison identified the constitutive differences between 'Ariane' and 'Roho' at the beginning of the storage period. A general clustering heatmap of all the differentially expressed genes (DEGs) was produced and analyzed, showing well defined groups of genes with different expression patterns (Fig. 2A). The number of DEGs identified in each comparison was similar, going from 2137 DEGs in AI *vs.* AC to 2627 DEGs in RD *vs.* RC (Fig. 2B; Tab S1). The percentage of up-regulated genes was 41.2%, 39.6% and 39.8% in AI *vs.* AC, RI *vs.* RC and RD *vs.* RC respectively, with only RC *vs.* AC showing more than 50% of up-regulated genes (57.6%) (Fig. 2B). According to the Venn diagram (Fig. 2C), only 199 genes resulted as regulated in all the comparisons (3.6%), while those specifically regulated in one comparison were 662 for AI *vs.* AC (11.8%), 268 for RI *vs.* RC (4.8%), 346 for RD *vs.* RC (6.2%) and 1556 for RC *vs.* AC (27.8%).

The accuracy of the RNA-Seq approach was tested by reverse transcription quantitative PCR (RT-qPCR). Ten differentially expressed genes were selected, and specific primers were designed for each gene (Tab S2). The expression level obtained by RT-qPCR was compared to the one estimated by RNA-Seq (Fig. 3A). A correlation analysis was performed, and a significant positive correlation (with Pearson correlation coefficient $R^2 = 0.7488$) between the DEGs expression level evaluated with RNA-Seq and RT-qPCR validated the RNA-Seq data (Fig. 3B).

Kyoto Encyclopedia of Genes and Genomes (KEGG) enrichment analyses were performed for the DEGs identified in the four pairwise comparisons, and the top 20 enriched categories for each one were shown in Fig. 4. 'Plant hormone signal transduction' was among the most enriched categories in all the comparisons, together with 'Biosynthesis of secondary metabolites' and 'Metabolic pathways' (Fig. 4). 'Starch and sugar metabolism' and 'Limonene and pinene degradation' were present in three of the four comparisons, while 'Linoleic acid metabolism' were present in AI *vs.* AC and RI *vs.* RC (Fig. 4). A specific enrichment was observed for KEGG categories enriched in only one comparison, such as 'Photosynthesis' in AI *vs.* AC (Fig. 4C) and 'beta-Alanine metabolism' in RC *vs.* AC (Fig. 4D). 'Monoterpenoid metabolism' resulted highly enriched in RI *vs.* RC and RD *vs.* RC (Figs. 4B, 4C).

Gene Ontology (GO) enrichment analyses for the four DEGs lists

Table 1
RNA-seq data elaboration statistics. For each RNA library, the amount of paired-end raw reads, the number and the percentage of paired reads survived to filtering, and the number and the percentage of paired reads aligned to apple reference genome were reported.

Sample properties				*Filtering*		*Aligning to genome*	
Cultivar	**Treatment**	**Sample ID**	**Input read pairs**	**N° pairs survived**	**% pairs survived**	**N° aligned pairs**	**% aligned pairs**
Ariane	Control	AC1	36,682,140	35,163,000	95.86%	32,770,110	93.19%
		AC2	39,856,783	38,525,467	96.66%	35,902,458	93.19%
		AC3	35,601,563	34,353,212	96.49%	31,960,115	93.03%
Ariane	Inoculated, no symtoms	AI1	46,372,322	44,494,660	95.95%	41,288,831	92.80%
		AI2	42,360,759	40,904,763	96.56%	38,065,269	93.06%
		AI3	52,584,974	50,587,369	96.20%	47,130,526	93.17%
Roho	Control	RC1	45,236,912	43,404,246	95.95%	40,591,890	93.52%
		RC2	49,303,051	46,603,247	94.52%	43,662,358	93.69%
		RC3	46,897,198	45,110,168	96.19%	42,313,084	93.80%
Roho	Inoculated, no symtoms	RI1	46,785,730	45,066,728	96.33%	41,604,572	92.32%
		RI2	42,629,395	41,207,043	96.66%	38,378,466	93.14%
		RI3	46,610,696	44,559,159	95.60%	40,295,063	90.43%
Roho	Inoculated, diseased	RD1	47,253,454	45,518,744	96.33%	42,018,173	92.31%
		RD2	51,458,994	49,728,763	96.64%	46,198,445	92.90%
		RD3	46,479,010	44,900,772	96.60%	42,060,326	93.67%

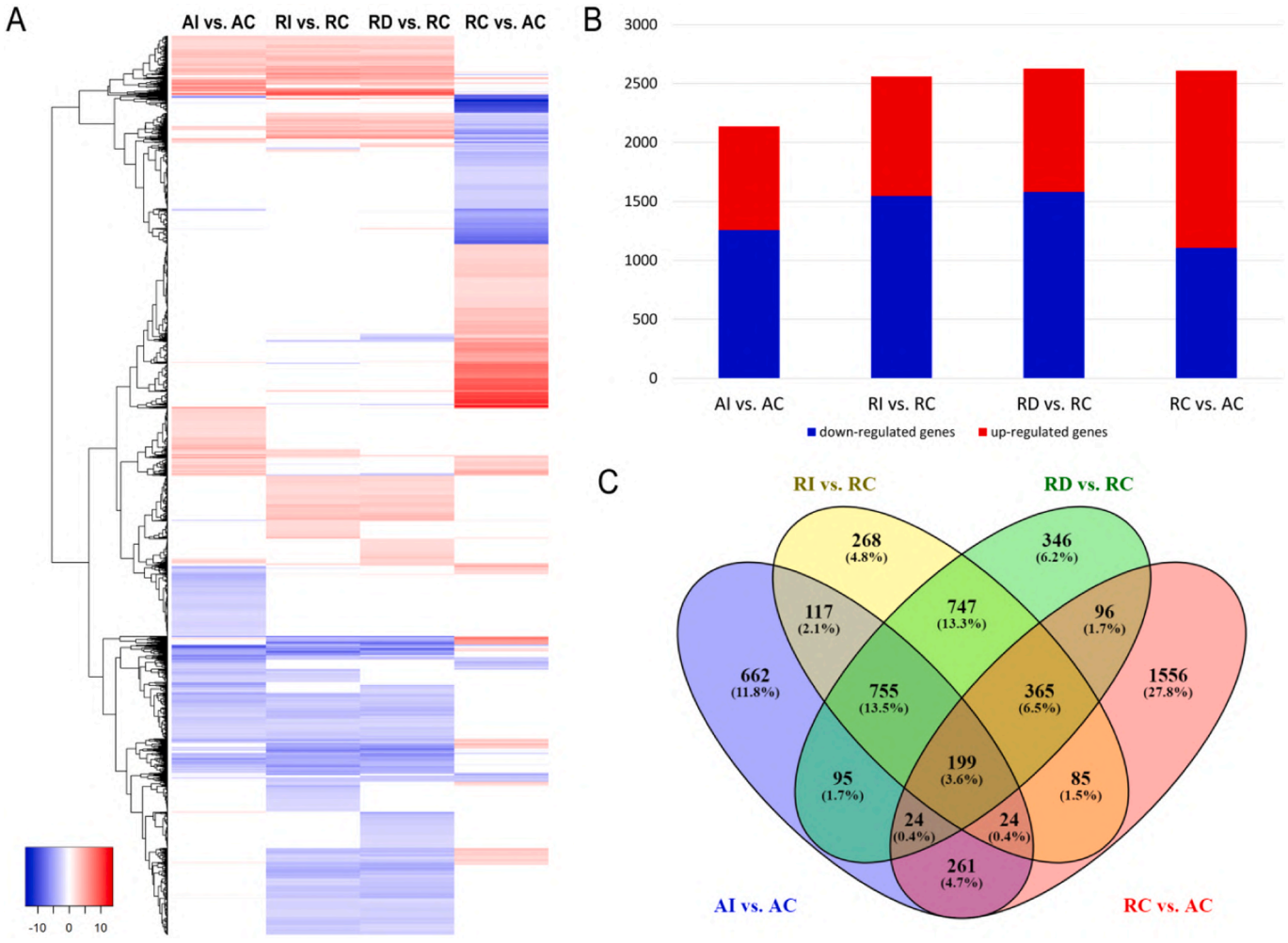

Fig. 2. Differential expression analysis results. A. General clustering heatmap of all the differentially expressed genes (DEGs) for AI *vs.* AC, RI *vs.* RC, RD *vs.* RC and RC *vs.* AC pairwise comparisons; color key was displayed. B. Bar plot visualizing the total number of DEGs identified in the AI *vs.* AC, RI *vs.* RC, RD *vs.* RC and RC *vs.* AC comparisons; the number of down-regulated (blue bars) and up-regulated DEGs (red bars) was also displayed. C. Venn diagram of DEGs from the four pairwise comparisons; the number and the percentage of DEGs included in each class were reported.

showed that 'Oxidation reduction' was the main category enriched in all the comparisons, while 'Response to biotic stimulus' was significantly enriched in RI *vs.* RC and RD *vs.* RC (Tab. S3). Interestingly, 'defense response' and 'Response to stress' were the two main categories enriched in RC *vs.* AC (Tab. S3).

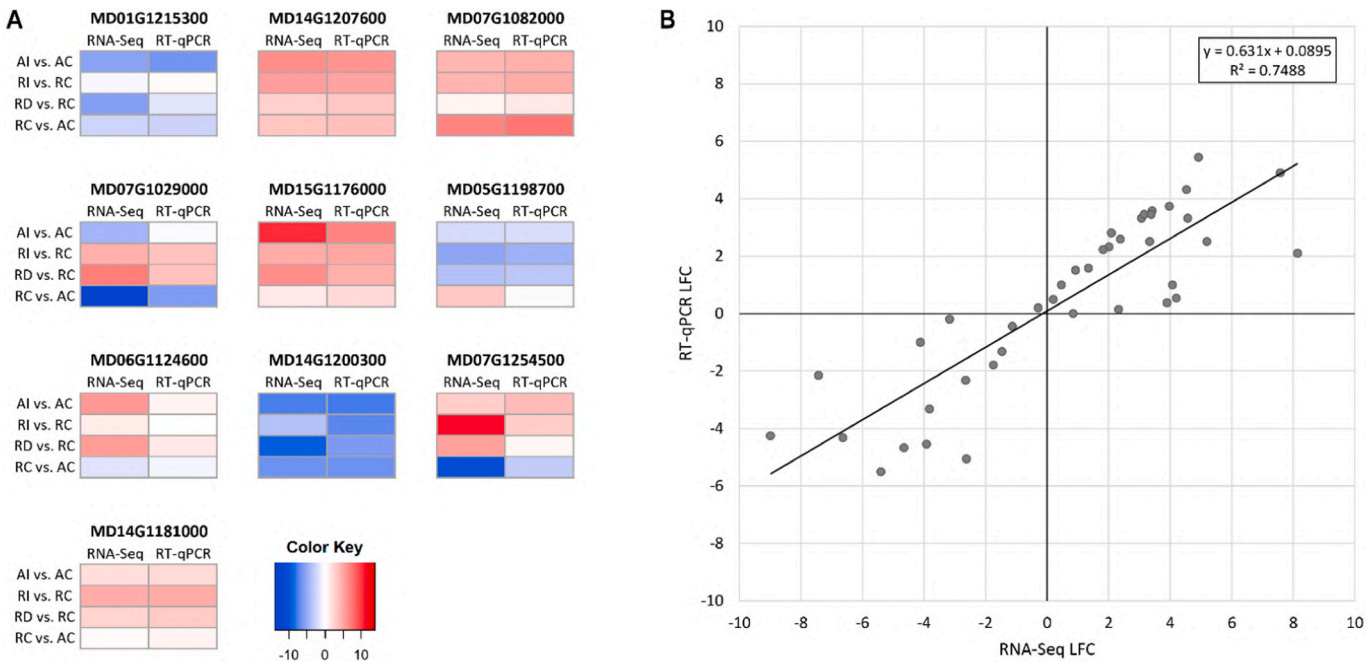

Fig. 3. RNA-Seq data validation by RT-qPCR. A. Heatmaps of ten genes $\log_2$(Fold Change) values estimated by RNA-Seq and RT-qPCR for AI *vs.* AC; RI *vs.* RC; RD *vs.* RC and RC *vs.* AC pairwise comparisons; color key was displayed. B. Correlation analysis between RNA-Seq and RT-qPCR $\log_2$(Fold Change) values; data points represent the $\log_2$(Fold Change) values resulting from RNA-Seq (X axis) and RT-qPCR (Y axis) analyses for each gene and comparison; the regression line equation and the Pearson correlation coefficient R^2 were displayed.

3.3. Pathogen-related DEGs

Several classes of genes related to plant-pathogen interaction were found to be regulated in the four comparisons (Fig. 5; Fig. S2). Antioxidant enzymes were represented by peroxidases, superoxide dismutases and alkenal reductases (Fig. 5A). The majority of the peroxidases were repressed in 'Roho' after four months of storage in both healthy and diseased fruits, while the same number of induced and repressed transcripts was found in 'Ariane'. Constitutive differences were also found between the two cultivars, with several genes encoding for peroxidases more expressed in RC or in AC. A different situation was found for superoxide dismutases, which were regulated in RD fruits only, except for MD12G1231900 gene, which was induced also in AI (Fig. 5A). Interestingly, no constitutive differences between the two cultivars were found for this class of enzymes. The regulation of alkenal reductase enzymes was quite similar after storage in both genotypes, with some exceptions: MD15G1173400 was up-regulated only in RI and RD, while MD15G1145600 was up-regulated only in RD. Constitutive differences were also found, as observed in the case of MD00G1045700, MD02G1002100 and MD16G1282000.

Enzymes directly involved in pathogen cell wall disruption, such as chitinase and GDSL esterase, were found regulated after 4 months of storage. Surprisingly, most of such enzymes were down-regulated in both cultivars (Figs. 5B and 5C). Moreover, the large majority of GDSL esterase showed a higher constitutive expression in the susceptible cultivar than in the resistant one. However, differential regulation between the two cultivars was found for both enzymes. For chitinase, MD02G1011100 was up-regulated, while MD01G1213100, MD02G1120300, MD04G1048000 and MD04G1150900 were down-regulated only in RI and RD (Fig. 5B). Regarding GDSL esterases, genotype-specific regulation was observed for most of the genes, except for MD09G1033000, MD14G1164400, MD16G1100400 and MD17G1180300 that were down-regulated in both 'Roho' and 'Ariane' after storage (Fig. 5C). Glutahione s-transferase enzymes were also found largely down-regulated in both cultivars, with many genes showing specific regulation in different comparisons (Fig. 5D). MD02G1204200 and MD04G1112100 were down-regulated only in 'Ariane'; MD04G1139500 was up-regulated only in 'Ariane'; MD16G1081100 and MD17G1260600 were down-regulated in both healthy and diseased 'Roho' fruits; MD02G1236100 and MD04G1111400 was down-regulated only in RD; MD02G1204400 was down-regulated only in RI, and MD12G1129400 was up-regulated in AI and RI (Fig. 5D). Another class of enzymes involved in pathogen defense include carboxylesterase and methylesterase genes. Genotype-specific differences were found for both categories (Fig. 5E). In particular, for carboxylesterase, MD09G1086100 was found to be expressed at the same level in AC and RC, but strongly up-regulated after four months of storage only in the resistant cultivar (Fig. 5E).

Another important class of genes that was shown to be involved in plant response to pathogen is represented by the heat shock proteins (HSPs). Once again, most of the HSPs regulated during storage showed a decreased expression level when compared to control fruits in both 'Ariane' and 'Roho'. Some transcripts showed genotype-specific regulation, such as MD02G1171800 and MD07G1196800, specifically up-regulated in 'Ariane' after storage, MD09G1271100, specifically up-regulated in RI and RD, and MD08G1068700, specifically up-regulated only in RD (Fig. 5F). For the down-regulated genes, MD13G1108500 expression was reduced only in AI; MD11G1088300 and MD15G1053800 were down-regulated only in RD; MD03G1213300 was down-regulated only in RI; MD08G1068200 was down-regulated in AI and RI, while MD07G1210700 in AI and RD (Fig. 5F). Similarly to GDSL esterase, many HSPs showed a higher constitutive expression in the susceptible cultivar than in the resistant one. A class of pathogen-related genes that showed a clear genotype-related regulation was represented by the mitogen-activated protein kinases (MAPKs). MAPKs were found to be up-regulated only in 'Roho', with MD02G1173600, MD05 G1349600, MD06G1101300, MD11G1070200 and MD15G1285100 genes up-regulated in both diseased and healthy fruits, and MD03G1065400 up-regulated only in RI (Fig. 5G). In 'Ariane', a single down-regulated gene was found, MD06G1089500.

Several other classes of genes related to plant-pathogen interaction showed differential levels of gene expression after storage. Ninety-eight

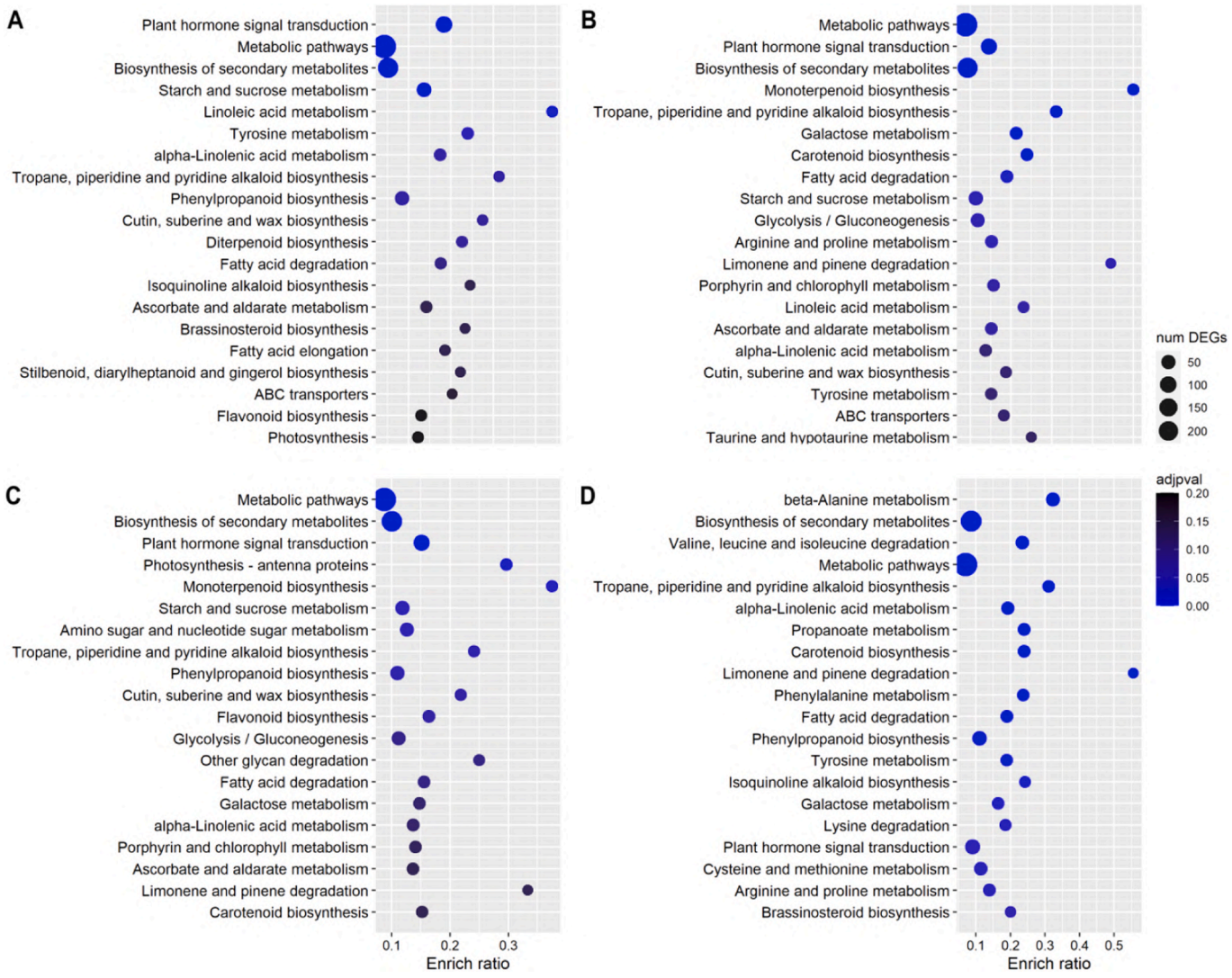

Fig. 4. KEGG enrichment bubble diagrams displaying the top 20 enriched KEGG categories of AI *vs.* AC (A), RI *vs.* RC (B), RD *vs.* RC (C) and RC *vs.* AC (D) pairwise comparisons. X axis represent the enrichment ratio (number of DEGs belonging to the KEGG category / number of genes belonging to the same KEGG category in the background genome); Y axis represent the enriched KEGG categories ordered by the number of detected DEGs; the dots size represents the numbers of DEGs included in each KEGG category; the dots color represents the adjusted *p*-value for each KEGG category enrichment.

leucine rich repeat (LRR) sequences were found to be regulated in one or more comparisons, showing differences in both constitutive and induced expression regulation (Fig. S2A). Similarly, 103 genes showing homology to different types of disease resistance proteins were shown to be regulated (Fig. S2B). Other regulated genes involved in plant-pathogen interaction include 13 members of the WRKY transcription factors gene family (Fig. S2C) and some homologs to susceptibility genes such as *MLO* and *DMR6* (Fig. S2D and S2E).

3.4. Ripening and stress-related DEGs

The ripening process can modify the physical and biological properties of apple fruits, possibly influencing the pathogen development. Therefore, the expression level of several classes of genes related to such process was examined. Several ethylene-responsive transcription factors were found to be differentially regulated in the two cultivars (Fig. 6A). Although, as expected, the expression level of most of these genes was enhanced after storage, several examples of genotype-specific regulation were found. MD02G1096500, MD02G1176200, MD02G1217900, MD05G1311400 and MD15G1326800 genes were up-regulated in RI and RD; MD07G1284200 was up-regulated only in RI and MD09G1228500 only in RD, while it was down-regulated in AI. MD06G1051900 and MD07G1248600 were up-regulated only in AI (Fig. 6A). A more diverse situation was found for abscisic acid (ABA)-responsive genes, with a similar number of up- and down-regulated genes (Fig. 6B). For this class of genes, the only constitutive differences between 'Ariane' and 'Roho' were represented by es MD04G1165000 and MD12G1178800, homologous to an ABA receptor, that were expressed at much higher level in RC than in AC. After storage, the expression of both genes was strongly down-regulated in RI and RD, while no regulation was observed in AI (Fig. 6B). Numerous auxin-responsive genes were also found to be regulated in both 'Ariane' and 'Roho' (Fig. 6C). In this case, the two cultivars showed quite different behaviors. A lot of genes were expressed at lower level in RC than in AC but, after storage, in 'Ariane' most of them were down-regulated, while in 'Roho' both up- and down-regulated genes were found (Fig. 6C).

Several classes of transcription factors known to be involved in fruit ripening and stress response processes were examined. Thirty-one members of the NAC domain-containing transcription factors family were found to be differentially expressed in one or more comparisons (Fig. 6D). In this group, the regulation of MD01G1093900 and MD01G1094000 genes was particularly interesting. These genes were

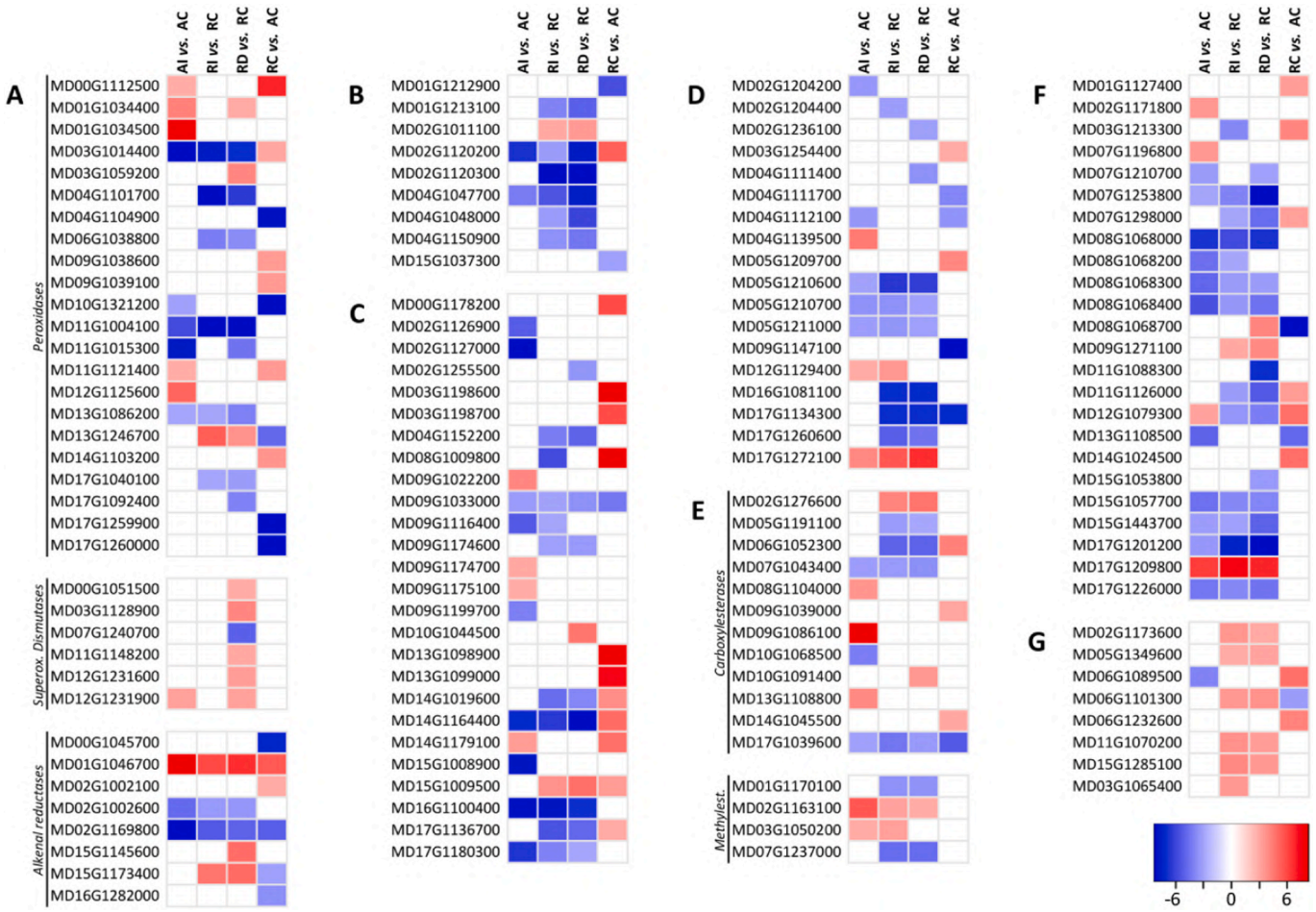

Fig. 5. Heatmaps visualizing the $\log_2$ Fold Change (LFC) values for pathogen-related DEGs resulting from the four comparisons AI *vs.* AC; RI *vs.* RC; RD *vs.* RC and RC *vs.* AC. DEGs were grouped according to their class: antioxidant enzymes (A, labeled as 'peroxidases', 'superoxide dismutases' and 'alkenal reductases'); chitinase (B); GDSL esterase(C); glutathione s-transferase (D); carboxylesterase and methylesterase (E); HSPs (F); MAPKs (G). For each class, genes were sorted in alphabetical order. Color key was displayed.

expressed at the same level in AC and RC, but showed completely different behavior after 4 months of storage: in AI they were up-regulated, in RD they were down-regulated, while no significant variation in expression level was observed in RI (Fig. 6D). Another gene (MD06G1121400) was expressed at much lower level in RC than in AC, but it was strongly up-regulated in both RI and RD, while no expression variation was found in AI (Fig. 6D). Most of the transcription factors belonging to the bHLH family were found to be down-regulated in both cultivars after storage, with few exceptions: MD01G1155000 was up-regulated in AI, MD05G1302400 was up-regulated in RD, MD13G1047100 was up-regulated in AI and RD and MD16G1247600 in AI and RI (Fig. 6E). Numerous zinc finger domain-containing proteins were found to be regulated in both 'Ariane' and 'Roho' (Fig. 6F). Many of them showed genotype-specific regulation. In particular, MD02G1162100, MD03G1206000, MD07G1265700, MD12G1051900, MD15G1315200 and MD16G1148500 genes were expressed at much higher level in RC than in AC. Nevertheless, none of these genes resulted regulated after four months of storage (Fig. 6F). Finally, the stress-responsive family of late embryogenesis abundant proteins (LEA) showed a distinct down-regulation only in RD fruits (Fig. 6G), with the only exception of MD06G1094300 that was down-regulated also in RI.

3.5. VOCs profiles

Five apples for each cultivar and condition (AC; RC; AI; RI and RD) were randomly selected and used for VOCs analyses. The aroma profiles of apples were non-invasively measured using PTR-ToF-MS. The high analytical sensitivity of this instrument allows the untargeted evaluation of the entire volatile composition of the fruit, also including compounds present at trace levels.

The first two principal components (PC1 and PC2) of the PCA (Figs. 7A and 7B), performed on the VOCs significantly different from the blank, explained 73.4% of the variability between apple categories. As also showed in the heatmap (Fig. 7C), the major difference between the aroma profiles of these samples were mostly due to the ripening of the fruit during the postharvest period ("C" vs. "I"). This change can be associated with the variation in PC1 values (53.3%). In contrast, the variability explained by the second principal component (PC2: 19.9%) is related to differences in the flavor profile of the two cultivars, especially at the time before inoculation (Fig. 7). Based on the cluster analysis of all VOC mass peaks (Fig. 7C), three main clusters are highlighted, the second of which is closely related to the VOC profile of damaged infected apples (RD). More in detail, after storage, tentatively identified (t.i.) ethanol (m/z 47.0487), methanol (m/z 33.0334), acetaldehyde (m/z 45.033), ethyl acetate (m/z 89.0597), formaldehyde (m/z 31.0182) and furan (m/z 69.0346) were the main volatiles produced at higher level by the diseased 'Roho' fruits (Fig. 7C and Fig. 8). Minor differences were found for styrene (m/z 105.0750), while slightly higher emission of t.i. hexenal (m/z 99.0799) and C10 esters (m/z 173.1522) was recorded for 'Ariane' (Fig. 8).

As for the constitutive differences in VOCs emission at the beginning of the storage period, numerous compounds were emitted at higher level

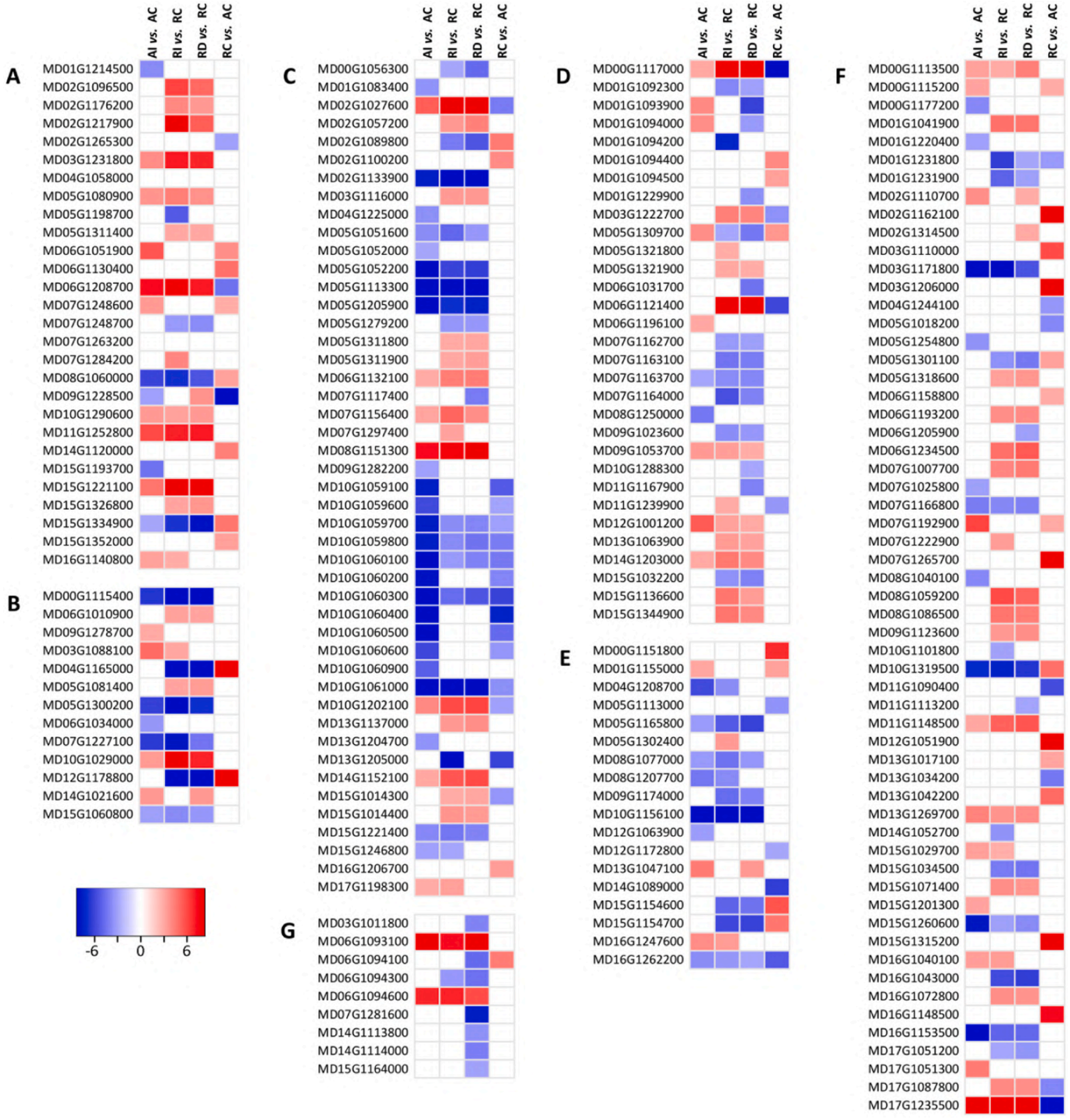

Fig. 6. Heatmaps visualizing the $\log_2$ Fold Change (LFC) values for stress-related genes resulting from the four comparisons AI *vs.* AC; RI *vs.* RC; RD *vs.* RC and RC *vs.* AC. DEGs were grouped according to their class: ethylene-responsive transcription factors (A); ABA-responsive genes (B); auxin-responsive genes (C); NAC transcription factors (D); bHLH transcription factors (E); zinc finger domain-containing proteins (F); LEA (G). For each class, genes were sorted in alphabetical order. Color key was displayed.

by RC when compared to AC, such as t.i. butenol (*m/z* 55.0542), propenal (*m/z* 57.0334), butenal (*m/z* 71.0491), C5 alcohol (*m/z* 71.0855), ethyl acetate (*m/z* 89.0597), phenylethanol (*m/z* 123.0818) and different types of esters (*m/z* 103.0753; 117.091; 131.1058; 159.1369) (Fig. 8). A peculiar case was represented by t.i. methyl acetate (*m/z* 75.044) that was constitutively emitted at higher level by 'Roho' at the beginning of the storage period; then, after four months of storage, the level remained high in diseased fruits, while in healthy 'Roho' it significantly decreased and in 'Ariane' remained quite low (Fig. 8).

4. Discussion

4.1. Transcriptome regulation during *N. vagabunda* infection

N. vagabunda infects apples during the growing season, but remains quiescent for a long time. Symptoms of BER may appear on susceptible fruits after several weeks or even months of post-harvest storage, and the growth of the fungus is probably triggered by compounds produced by the fruit during the ripening process, such as ethylene (Cameldi et al.,

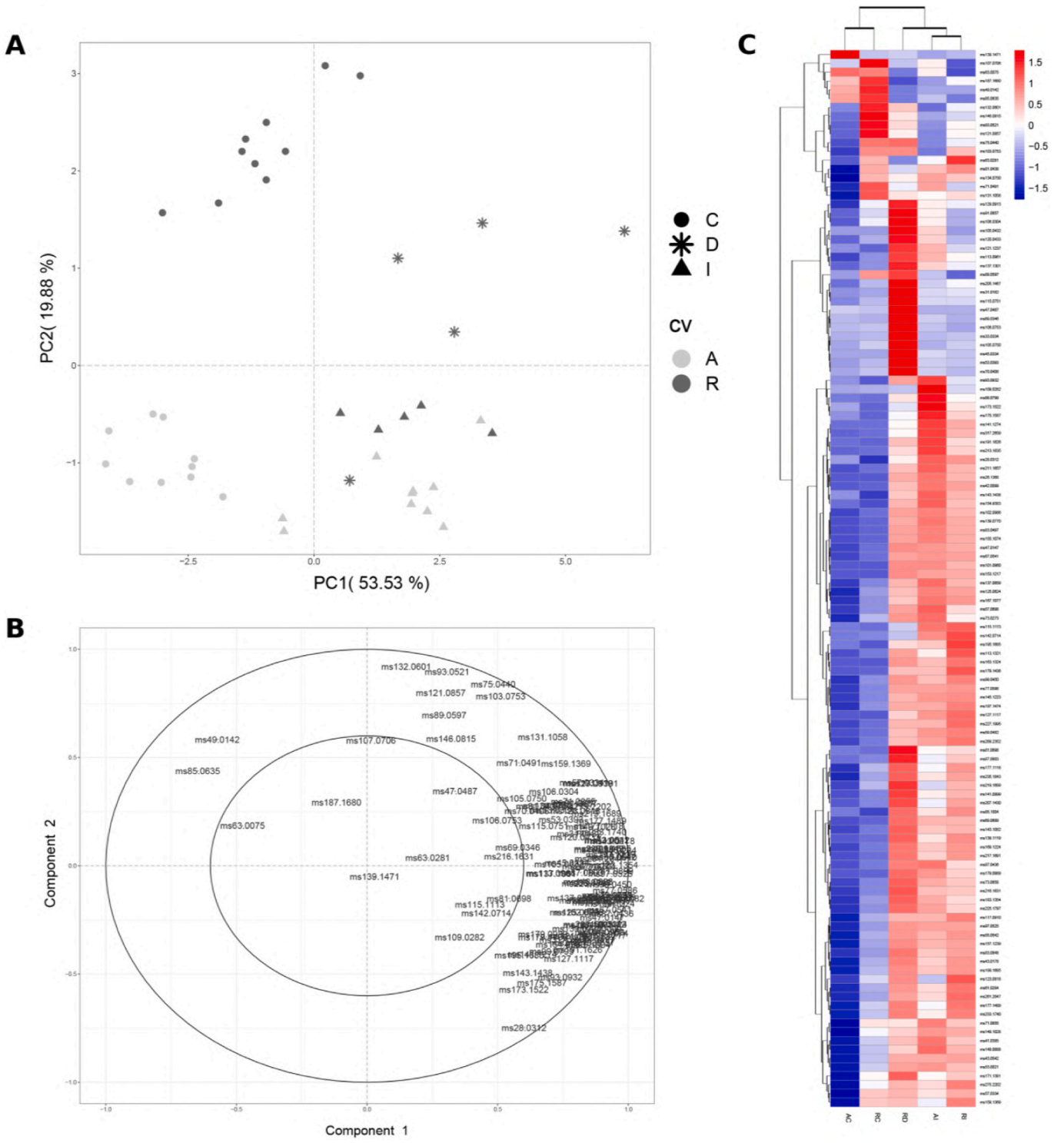

Fig. 7. Results of PTR-ToF-MS analysis. PCA (A), loading plot (B) and heatmap with two dimensional hierarchical dendrograms (C) of the VOCs identified in 'Ariane' control fruits (AC); 'Ariane' fruits inoculated with *N. vagabunda* showing no symptoms (AI); 'Roho' control fruits (RC); 'Roho' fruits inoculated with *N. vagabunda* showing no symptoms (RI) and diseased 'Roho' fruits (RD) were displayed. Color key was reported.

2016). Therefore, it is difficult to determine exactly when the actual infection takes place. Moreover, as shown by our results, not all the infected fruits develop symptoms, and this makes it quite challenging to study the gene expression during changes the fruit-pathogen interaction. Another limiting factor was the small number of fruits analyzed. For technical reasons, only one fruit per biological replicate was analyzed in the present study. A larger number of fruits per replicate would have provided more solidity to the statistical data, probably reducing the number of regulated genes. Nonetheless, RNA-Seq results allowed the identification of numerous gene classes which regulation seems associated to phenotypic differences, and 346 genes were found to be regulated only in diseased fruits. This putatively indicates the capability of the fruit to perceive *N. vagabunda* infection and even respond to it. After four months of storage at 4 °C, both 'Ariane' and 'Roho' (healthy and diseased) fruits showed a higher number of down-regulated genes than up-regulated ones, possibly indicating a gradual decrease in gene

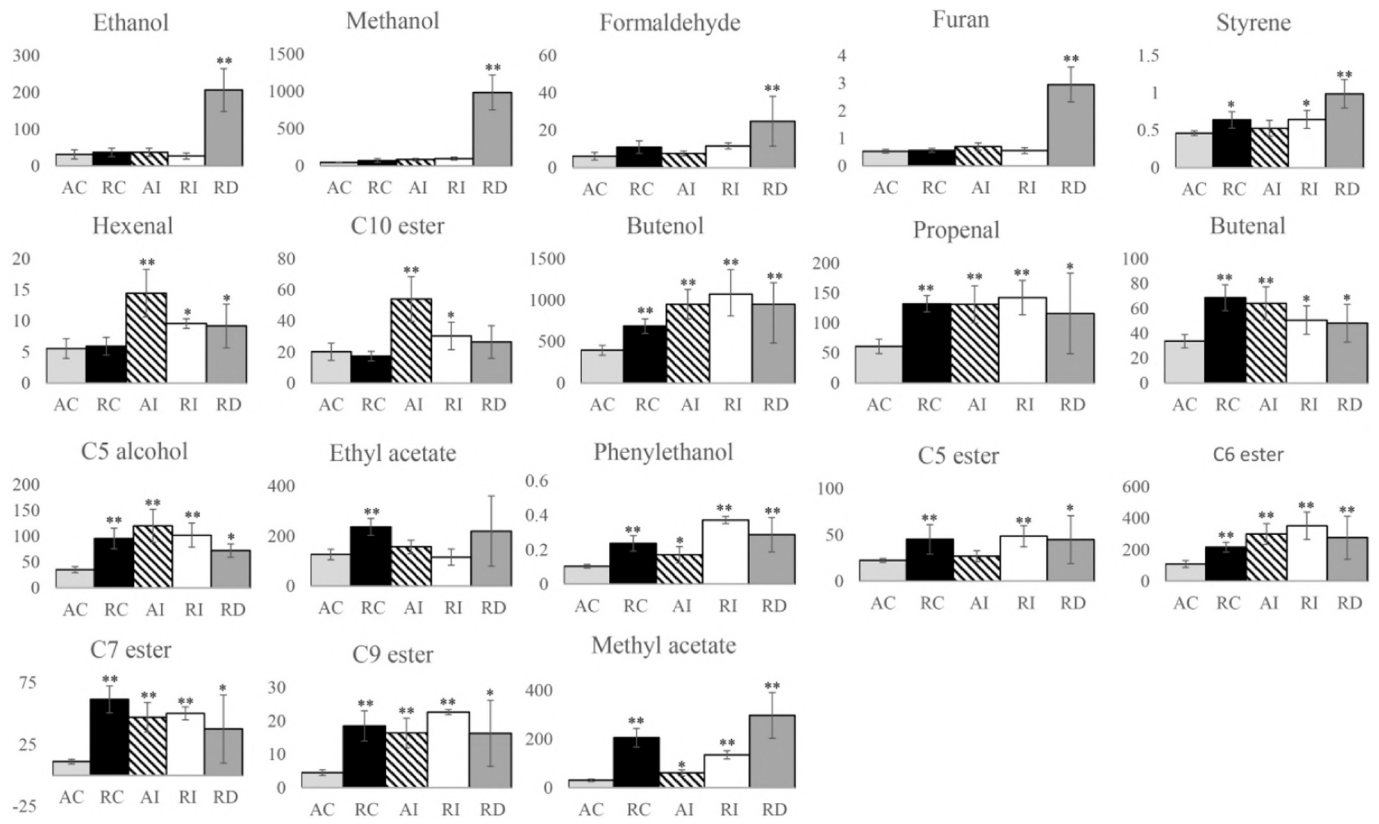

Fig. 8. Profile of specific volatiles in 'Ariane' control fruits (AC); 'Ariane' fruits inoculated with *N. vagabunda* showing no symptoms (AI); 'Roho' control fruits (RC); 'Roho' fruits inoculated with *N. vagabunda* showing no symptoms (RI) and diseased 'Roho' fruits (RD). For each compound, the t.i. name is reported. Ethanol (*m/z* 47.0487; C2H6OH+); methanol (*m/z* 33.0334; CH4OH+); formaldehyde (*m/z* 31.0182; CH2OH+); furan (*m/z* 69.0346; C4H4OH+); styrene (*m/z* 105.0750; C8H9+); hexenal (*m/z* 99.0799; C6H10OH+); C10 esters (*m/z* 173.1522; C10H20O2H+); butenol (*m/z* 55.0542; C4H7+); propenal (*m/z* 57.0334; C3H4OH+); butenal (*m/z* 71.0491; C4H6OH+); C5 alcohol (*m/z* 71.0855; C5H11+); ethyl acetate (*m/z* 89.0597; C4H8O2H+); phenylethanol (*m/z* 123.0818; C8H10OH+); C5 esters (*m/z* 103.0753; C5H10O2H+); C6 esters (117.091; C6H12O2H+); C7 esters (131.1058; C7H14O2H+); C9 esters (159.1369; C9H18O2H+); methyl acetate (*m/z* 75.044; C3H6O2H+). The amount of each compound (*y* axis) is expressed in ppb_v of the most representative mass peak evaluated by using PTR-ToF-MS. Significant differences between means are indicated, referred to AC (*p<0.05; **p<0.01).

transcription as a natural consequence of the ongoing ripening process of a detached fruit, but also a lower fruit metabolism possibly due to the low storage temperature itself. When studying gene expression during a long period of storage, an important and challenging issue is to distinguish between genes that are regulated by the pathogen-host interaction and all the other genes that are physiologically regulated during fruit ripening/senescence (i.e., sugars and cell wall modifications). KEGG and GO analysis showed that pathways related to starch and sugar metabolism were significantly enriched in DEGs in most of the comparisons but, while changes in sugar content have been previously correlated to pathogen infection, it is also well known that such modifications are typical of the ripening process (Chen et al., 2018; Žebeljan et al., 2019). Moreover, genotype-related differences in starch and sugar content can influence the genetically determined resistance to storage rots (Nybom et al., 2020).

4.2. Pathogen-related genes

When pathogen-related classes of genes were considered, a large number of regulated sequences was often found, as in case of LRR genes or disease resistance proteins. According to our results, several classes of genes could be highlighted to play a putative role in pathogen response. Two classes of genes directly involved in pathogen cell wall disruption, chitinase and GDSL esterase, were found surprisingly down-regulated in both 'Ariane' and 'Roho'. Chitinase are enzymes hydrolyzing the N-acetylglucosamine polymer chitin, a component of the cell wall of fungi. They are often expressed at low level, but can be dramatically up-regulated during pathogen infection. Their role in pathogen resistance is well documented in apple (Haxim et al., 2022). Similarly, GDSL esterase are lipolytic enzymes capable of hydrolyzing pathogen cell wall or membrane (Shen et al., 2022). In Arabidopsis, a GDSL esterase was found to be involved in the resistance to the necrotrophic fungus *Alternaria brassicicola* (Oh et al., 2005). The fact that most of the members of these families were found down-regulated in both 'Ariane' and 'Roho' may indicate that, after a long period of storage, apple fruits gradually decrease their ability to respond to biotic stress. Nonetheless, some members of the GDSL esterase family were actually up-regulated in one of the two cultivars, so the possibility that this was due to a specific response to *N. vagabunda* cannot be ruled out. The higher expression level of GDSL esterase genes found in the susceptible cultivar 'Roho' at harvest suggests that these enzymes are not enough, per se, to protect the fruit from fungi infections. Glutathione s-transferase gene family was also found largely down-regulated after 4 months of storage in both cultivars. This was less surprising than for chitinase and GDSL esterase, as glutathione s-transferase is a vast family of multifunctional enzymes involved in different processes (Gullner et al., 2018). Therefore, the attention should be focused only on specifically up-regulated members, such as MD04G1139500, MD12G1129400 and MD17G1272100. The same is true also for carboxylesterase and methylesterase genes, hydrolytic enzymes that act on carboxylic esters and are involved in numerous metabolic processes, going from plant growth and specialized metabolites synthesis to plant defense response (Cao et al., 2019). Of particular interest was the case of a carboxylesterase gene (MD09G1086100), whose expression was strongly up-regulated only in

the resistant cultivar 'Ariane'. Further experiments are needed, in order to assess the involvement of MD09G1086100 in pathogen response.

Production of reactive oxygen species (ROS), or oxidative burst, is one of the main responses of plants to pathogen infections, and it is known to occur also in case of fruit post-harvest infections(Bui et al., 2019). However, the excess of ROS can be harmful also for the fruit itself, damaging DNA, lipids and proteins. Therefore, after the oxidative burst, antioxidant enzymes are produced in order to modulate ROS homeostasis by both pathogen and host. The balance between ROS production and scavenging may have a deep impact on the final outcome of the infection (Camejo et al., 2016). According to our results, different classes of antioxidant enzymes were regulated during fruit storage. In particular, superoxide dismutase gene family seemed to be induced only in RD, suggesting a specific involvement of this enzyme in fruit response to *N. vagabunda* infection. The role of superoxide dismutase and other antioxidant enzymes in apple fruit response to fungi was already suggested for *Penicillium expansum* (Jimdjio Kouasseu et al., 2023). Other classes of antioxidant enzymes, such as peroxidase and alkenal reductase, although regulated during the four months of storage in both cultivars, showed a less specific regulation. Nonetheless, some members of each family showed up-regulation in 'Ariane' or 'Roho', so their involvement in fruit interaction with *N. vagabunda* cannot be ruled out. Peroxidases are supposed to play a role in apple-pathogen interaction and can be produced by the pathogen and by the host (Feng et al., 2018).

HSPs represent a large family of chaperone proteins that were originally associated to an increase of temperature. Later, it was discovered that HSPs may play a role in numerous plant physiological responses (Ul Haq et al., 2019). Several classes of HSPs, such as HSP70 and HSP24 were shown to be involved in pathogen response (Berka et al., 2022; Li et al., 2021). According to our results, most of the HSPs were down-regulated after fruit storage, once again suggesting a general decrease in the efficiency of fruit defense mechanisms that could be exploited by the pathogen. Nonetheless, one member of HSP70 (MD07G1196800) and one of HSP24 (MD02G1171800) were found to be specifically up-regulated in the resistant cultivar 'Ariane', indicating that they could be involved in fruit response to *N. vagabunda*.

A class of genes that showed clear differences between 'Ariane' and 'Roho' was the MAPK family. MAPKs are thought to mediate the early response of the plant to pathogen infection (Meng and Zhang, 2013). It was quite surprising to find six members of this family that were up-regulated in 'Roho' after a long period of storage, with the diseased fruits already showing large necrotic lesions. Moreover, the same MAPK genes were up-regulated even in 'Roho' fruits showing no visible symptoms of infection. One possible explanation is that in the resistant cultivar 'Ariane', following *N. vagabunda* recognition, an early and transient overexpression of MAPKs occurs, blocking the infection. In the susceptible cultivar 'Roho', the onset of fruit response could be much delayed, leading to a prolonged induction of MAPKs and to the development of BER symptoms. Differences in the onset of pathogen response was observed in apple for *Venturia inaequalis* infection, with reaction times ranging from 2 to 11 days(Bowen et al., 2011). If this is true, then the MAPKs induction in symptomless 'Roho' fruits may indicate that the infection of *N. vagabunda* was still in progress and the appearance of the symptoms simply delayed. A time-course experiment could be used to verify this hypothesis but, due to the long incubation of *N. vagabunda*, several time points would be necessary to appropriately monitor the infection during all the storage period.

4.3. Ripening and stress-related genes

During a long period of storage, apple fruits undergo through numerous changes, such as cell wall modifications (Peña and Carpita, 2004) and sugar and protein content variations (Johnston et al., 2002; Shi et al., 2014). All these changes may influence *N. vagabunda* infection development, so it is important to look for differences between resistant and susceptible cultivars, as well as between diseased and healthy fruits. Ethylene is one of the most studied phytohormone involved in the ripening process, and can influence fruit quality and storage life of apples (Payasi et al., 2009). According to our results, both 'Ariane' and 'Roho' showed a general induction of ethylene-responsive transcription factors (ERFs), as expected, while the ripening process progresses. Nonetheless, individual differences that can influence fruit characteristics and susceptibility to pathogens were highlighted, as a large number of ERFs exist, each with a different function. As an example, MD02G1217900 gene, which shows homology to *ERF34*, was up-regulated only in the susceptible cultivar 'Roho'. In Arabidopsis, *ERF34* was shown to mediate stress-induced leaf senescence (Park et al., 2022). On the other hand, MD06G1051900 gene was up-regulated only in the resistant cultivar 'Ariane'. MD06G1051900 is homologous to *ERF5*, that in Arabidopsis is involved in chitin-induced innate immunity response (Son et al., 2012), and therefore may play an important role in pathogen defense. Another hormone involved in fruit ripening is abscisic acid (ABA) (Fernández-Cancelo et al., 2022). Several ABA-related genes were found to be regulated during apple storage and, in this case, the individual differences seem to be more significant than the general trend of the whole gene family. MD04G1165000 and MD12G1178800 are both homologous to the ABA receptor *PYL4*, that was demonstrated to confer resistance to multiple abiotic stresses in Arabidopsis (Ren et al., 2022). Their expression was higher in the susceptible cultivar 'Roho' at the harvest time, but was dramatically down-regulated during the storage period, while no regulation was found in 'Ariane'. As for auxin, the content of indole-3-acetic acid (IAA, or free auxin) have been shown to decline in maturing fruits (Böttcher et al., 2010). Our results seem to be in accordance with such findings, with numerous auxin-induced genes being down-regulated after four months of storage in both 'Ariane' and 'Roho'. However, a genotype-dependent behavior seems to be present, with 'Roho' showing less down-regulated and more up-regulated genes. In apple, an ethylene-auxin crosstalk was recently proposed that could influence the postharvest ripening process in a cultivar-dependent way (Busatto et al., 2021). Other classes of transcription factors, known to be involved in biotic and abiotic stress response, that we found regulated during fruit storage include NAC, bHLH, zinc finger and WRKY families (Qian et al., 2021). Genotype-specific regulation of transcription factors was found at the harvest time or after storage in both 'Ariane' and 'Roho'. Due to the large number of genes belonging to each family and the many different functions they have in plants, it was quite difficult to identify specific candidates that could be involved in pathogen response. Nonetheless, in some cases, as for example the two NAC-like genes MD01G1093900 and MD01G1094000 genes, the transcriptional regulation during the storage period was found completely different in AI, RI and RD. This may be considered as a good indication that the interaction with *N. vagabunda* modulates the expression of these genes. In apple, it was recently found that infection with *Alternaria alternata* can modulate NAC transcription factors expression, with some members of the family that were up-regulated and others that were down-regulated (Li et al., 2020).

4.4. VOCs

The main VOCs whose production was found clearly increased during *N. vagabunda* infection of RD apple fruits were ethanol and methanol, in accordance with previous studies on *N. vagabunda* and *P. expansum* (Kim et al., 2018; Neri et al., 2019). Two other VOCs, furan and formaldehyde, were found up-regulated only in RD, even though their production was far less abundant than for ethanol and methanol. Emission of furan and formaldehyde by *N. vagabunda* was found also by Neri et al. (2019), but only during *in vitro* growth of the pathogen. According to our results, ethanol, methanol, furan and formaldehyde all seemed to be quite specific to diseased fruit, so they could be potential markers for *N. vagabunda* infection detection. Neri et al. (2019) also found an increase in C6 and C7 esters, such as ethyl hexanoate, ethyl

butanoate end ethyl-2-methyl-butanoate in rotten fruit when compared to healthy controls. According to our results, a comparable level of C6 and C7 esters was found in the resistant cultivar 'Ariane' as well as in the susceptible 'Roho' after four months of cold storage. Moreover, no significant differences were found between diseased and healthy fruits, suggesting that this class of compounds is not related to apple susceptibility to *N. vagabunda*.

Only two VOCs, hexenal and C10 esters were found induced at higher level in the resistant cultivar 'Ariane' after cold storage. Interestingly, hexenal was recently suggested as an important player during plant-fungi interaction, even though with contrasting results. In a recent study, hexenal was shown to reduce tomato susceptibility to *Botrytis cinerea* infection by modulating plant defense mechanisms (Zhang et al., 2023). Similarly, also postharvest fumigation of kiwifruit with hexenal enhanced resistance to *B. cinerea* (Hyun et al., 2022). On the other hand, another study seems to indicate that hexenal can facilitate *B. cinerea* infection in tomato and strawberry fruits by inducing sulfur assimilation in spores and hyphae of the fungus (Xu et al., 2021). In Arabidopsis, hexenal was found to enhance susceptibility to *Pseudomonas syringae* through the activation of the jasmonic acid pathway (Scala et al., 2013). Therefore, even if the role of hexenal could be quite complex, the involvement of this VOC in plant-fungi interaction appears evident.

The concentration of several VOCs was significantly higher in RC than in AC fruit. Nonetheless, most of them showed comparable emission level after four months of cold storage in both cultivars, and in both healthy and diseased fruits. The only exceptions were methyl acetate and C5 esters. In particular, methyl acetate is known to be involved in microbial interspecies communication and to inhibit the growth of several fungi and bacteria. For example, *Muscodor crispans*, an endophytic fungus of wild pineapple (*Ananas ananassoides*) can produce a mixture of VOCs capable to inhibit the growth of a wide range of plant pathogens, including the fungi *Phytium ultimum*, *Phytophtora cinnamomi*, *Sclerotinia sclerotiorum* and *Mycosphaerella fijiensis* (Mitchell et al., 2010). One of the main components of this mixture of VOCs is methyl acetate. Methyl acetate was shown to be the most active among the VOCs produced by another fungus of the *Muscodor* genus (*Muscodor albus*), capable of inhibiting the growth of several fungi and bacteria (Strobel et al., 2001). More recently, methyl acetate was shown to induce a strong down-regulation of the expression of most genes involved in the main metabolic functions of the bacterium *Serratia plymuthica* and play and important role in the interplay with the fungal plant pathogens *Leptosphaeria maculans* and *Verticillium longisporum* (Rybakova et al., 2022). According to our results, the concentration of methyl acetate in RD fruits was, on average, almost three times higher than in RI. This may indicate alternatively that: (i) the infection of *N. vagabunda* stimulates the fruit production of methyl acetate; (ii) *N. vagabunda* itself may produce methyl acetate during infection. In both cases, it could be of interest to study in more detail the role of this VOC.

5. Conclusions

The results presented in this work can be considered a first insight into the molecular mechanism regulating interaction between apple fruits and *N. vagabunda* during post-harvest storage. Our results indicate that apples are capable of perceiving *N. vagabunda* infection and modify gene expression accordingly. Even though apple fruits seemed to decrease their ability to respond to abiotic stress after a long period of storage, as indicated by the general down-regulation of chitinase and GDSL esterase, it was possible to identify several genes that may be involved in fruit-pathogen interaction. Some examples are superoxide dismutase genes and specific members of other families such as HSPs (MD07G1196800 and MD02G1171800), ERFs (MD06G1051900), carboxylesterases (MD09G1086100) and NAC transcription factors (MD01G1093900 and MD01G1094000). As for VOCs, our analyses seem to confirm that ethanol and methanol could be possible markers for *N. vagabunda* infection, as already suggested by other authors. Furan and formaldehyde seemed to be also quite specific markers, even though far less abundant. Comparison between a resistant and a susceptible cultivar allowed the identification of two VOCs, hexenal and methyl acetate, that could be involved in regulating apple-fungi interaction.

Funding

This work was supported by the Autonomous Province of Trento.

CRediT authorship contribution statement

Paolo Baldi: Writing – review & editing, Writing – original draft, Methodology, Investigation, Conceptualization. **Mickael Malnoy:** Writing – review & editing, Methodology. **Donatella Paffetti:** Data curation. **Franco Biasioli:** Writing – review & editing, Writing – original draft, Data curation. **Brian Farneti:** Writing – review & editing, Writing – original draft, Investigation, Data curation. **Iuliia Khomenko:** Writing – review & editing, Writing – original draft, Investigation. **Valeria Gualandri:** Writing – review & editing, Writing – original draft, Investigation. **Matteo Buti:** Writing – review & editing, Writing – original draft, Data curation, Conceptualization.

Declaration of Competing Interest

The authors declare that they have no known competing financial interests or personal relationships that could have appeared to influence the work reported in this paper.

Data availability

RNA-Seq raw reads data have been deposited and made available at EMBL-EBI under the accession number E-MTAB-13465.

Acknowledgments

The authors wish to thank Davide Busetti for orchard maintenance and fruit storage.

Appendix A. Supporting information

Supplementary data associated with this article can be found in the online version at doi:10.1016/j.postharvbio.2024.112889.

References

Berka, M., Kopecká, R., Berková, V., Brzobohatý, B., Černý, M., 2022. Regulation of heat shock proteins 70 and their role in plant immunity. J. Exp. Bot. 73, 1894–1909. https://doi.org/10.1093/jxb/erab549.

Bolger, A.M., Lohse, M., Usadel, B., 2014. Trimmomatic: a flexible trimmer for Illumina sequence data. Bioinformatics 30, 2114–2120. https://doi.org/10.1093/bioinformatics/btu170.

Böttcher, C., Keyzers, R.A., Boss, P.K., Davies, C., 2010. Sequestration of auxin by the indole-3-acetic acid-amido synthetase GH3-1 in grape berry (*Vitis vinifera* L.) and the proposed role of auxin conjugation during ripening. J. Exp. Bot. 61, 3615–3625. https://doi.org/10.1093/jxb/erq174.

Bowen, J.K., Mesarich, C.H., Bus, V.G.M., Beresford, R.M., Plummer, K.M., Templeton, M.D., 2011. *Venturia inaequalis*: the causal agent of apple scab. Mol. Plant Pathol. 12, 105–122. https://doi.org/10.1111/j.1364-3703.2010.00656.x.

Bu, D., Luo, H., Huo, P., Wang, Z., Zhang, S., He, Z., Wu, Y., Zhao, L., Liu, J., Guo, J., Fang, S., Cao, W., Yi, L., Zhao, Y., Kong, L., 2021. KOBAS-i: Intelligent prioritization and exploratory visualization of biological functions for gene enrichment analysis. Nucleic Acids Res 49, W317–W325. https://doi.org/10.1093/nar/gkab447.

Bui, T.T., Wright, S.A., Falk, A.B., Vanwalleghem, T., Van Hemelrijck, W., Hertog, M.L., Keulemans, J., Davey, M.W., 2019. *Botrytis cinerea* differentially induces postharvest antioxidant responses in 'Braeburn' and 'Golden Delicious' apple fruit. J. Sci. Food Agric. 99, 5662–5670. https://doi.org/10.1002/jsfa.9827.

Busatto, N., Tadiello, A., Moretto, M., Farneti, B., Populin, F., Vrhovsek, U., Commisso, M., Sartori, E., Sonego, P., Biasioli, F., Costa, G., Guzzo, F., Fontana, P., Engelen, K., Costa, F., 2021. Ethylene-auxin crosstalk regulates postharvest fruit ripening process in apple. Fruit. Res. 1, 1–13. https://doi.org/10.48130/FruRes-2021-0013.

Buti, M., Sargent, D., Velasco, R., Colgan, R., 2018. A study of gene expression changes at the Bp-2 locus associated with bitter pit symptom expression in apples (*Malus pumila*). Mol. Breed. 38, 85. https://doi.org/10.1007/s11032-018-0840-z.

Camejo, D., Guzmán-Cedeño, Á., Moreno, A., 2016. Reactive oxygen species, essential molecules, during plant-pathogen interactions. Plant Physiol. Biochem. 103, 10–23. https://doi.org/10.1016/j.plaphy.2016.02.035.

Cameldi, I., Neri, F., Ventrucci, D., Ceredi, G., Muzzi, E., Mari, M., 2016. Influence of harvest date on bull's eye rot of 'cripps pink' apple and control chemical strategies. Plant Dis. 100, 2287–2293. https://doi.org/10.1094/PDIS-05-16-0615-RE.

Cameldi, I., Neri, F., Menghini, M., Pirondi, A., Nanni, I.M., Collina, M., Mari, M., 2017. Characterization of *Neofabraea vagabunda* isolates causing apple bull's eye rot in Italy (Emilia-Romagna region). Plant Pathol. 66, 1432–1444. https://doi.org/10.1111/ppa.12684.

Cao, X., Duan, W., Wei, C., Chen, K., Grierson, D., Zhang, B., 2019. Genome-wide identification and functional analysis of carboxylesterase and methylesterase gene aamilies in peach (*Prunus persica* L. Batsch). Front. Plant Sci. 10, 473630 https://doi.org/10.3389/fpls.2019.01511.

Chen, Y., Grimplet, J., David, K., Castellarin, S.D., Terol, J., Wong, D.C.J., Luo, Z., Schaffer, R., Celton, J.M., Talon, M., Gambetta, G.A., Chervin, C., 2018. Ethylene receptors and related proteins in climacteric and non-climacteric fruits. Plant Sci. 276, 63–72. https://doi.org/10.1016/j.plantsci.2018.07.012.

Daccord, N., Celton, J.M., Linsmith, G., Becker, C., Choisne, N., Schijlen, E., Van De Geest, H., Bianco, L., Micheletti, D., Velasco, R., Di Pierro, E.A., Gouzy, J., Rees, D.J. G., Guérif, P., Muranty, H., Durel, C.E., Laurens, F., Lespinasse, Y., Gaillard, S., Aubourg, S., Quesneville, H., Weigel, D., Van De Weg, E., Troggio, M., Bucher, E., 2017. High-quality de novo assembly of the apple genome and methylome dynamics of early fruit development. Nat. Genet. 2017 497 (49), 1099–1106. https://doi.org/10.1038/ng.3886.

Di Francesco, A., Cameldi, I., Neri, F., Barbanti, L., Folchi, A., Spadoni, A., Baraldi, E., 2019. Effect of apple cultivars and storage periods on the virulence of *Neofabraea* spp. Plant Pathol. 68, 1525–1532. https://doi.org/10.1111/ppa.13074.

Farneti, B., Khomenko, I., Cappellin, L., Ting, V., Romano, A., Biasioli, F., Costa, G., Costa, F., 2015. Comprehensive VOC profiling of an apple germplasm collection by PTR-ToF-MS. Metabolomics 11, 838–850. https://doi.org/10.1007/s11306-014-0744-9.

Farneti, B., Khomenko, I., Grisenti, M., Ajelli, M., Betta, E., Algarra, A.A., Cappellin, L., Aprea, E., Gasperi, F., Biasioli, F., Giongo, L., 2017. Exploring blueberry aroma complexity by chromatographic and direct-injection spectrometric techniques. Front. Plant Sci. 8, 264825 https://doi.org/10.3389/FPLS.2017.00617/BIBTEX.

Farneti, B., Khomenko, I., Ajelli, M., Emanuelli, F., Biasioli, F., Giongo, L., 2022. Ethylene production affects blueberry fruit texture and storability. Front. Plant Sci. 13, 813863 https://doi.org/10.3389/FPLS.2022.813863/BIBTEX.

Feng, H., Zhang, M., Zhao, Y., Li, C., Song, L., Huang, L., 2018. Secreted peroxidases VmPODs play critical roles in the conidiation, H2O2 sensitivity and pathogenicity of *Valsa mali*. Fungal Genet. Biol. 119, 20–28. https://doi.org/10.1016/j.fgb.2018.08.003.

Fernández-Cancelo, P., Muñoz, P., Echeverría, G., Larrigaudière, C., Teixidó, N., Munné-Bosch, S., Giné-Bordonaba, J., 2022. Ethylene and abscisic acid play a key role in modulating apple ripening after harvest and after cold-storage. Postharvest Biol. Technol. 188, 111902 https://doi.org/10.1016/j.postharvbio.2022.111902.

Gullner, G., Komives, T., Király, L., Schröder, P., 2018. Glutathione S-transferase enzymes in plant-pathogen interactions. Front. Plant Sci. 871, 427485 https://doi.org/10.3389/FPLS.2018.01836/BIBTEX.

Haxim, Y., Kahar, G., Zhang, X., Si, Y., Waheed, A., Liu, X., Wen, X., Li, X., Zhang, D., 2022. Genome-wide characterization of the chitinase gene family in wild apple (*Malus sieversii*) and domesticated apple (*Malus domestica*) reveals its role in resistance to Valsa mali. Front. Plant Sci. 13, 1007936 https://doi.org/10.3389/fpls.2022.1007936.

Hyun, J., Lee, J.G., Yang, K.Y., Lim, S., Lee, E.J., 2022. Postharvest fumigation of (*E*)-2-hexenal on kiwifruit (*Actinidia chinensis* cv. 'Haegeum') enhances resistance to *Botrytis cinerea*. Postharvest Biol. Technol. 187, 111854 https://doi.org/10.1016/j.postharvbio.2022.111854.

Janisiewicz, W.J., Nichols, B., Bauchan, G., Chao, T.C., Jurick, W.M., 2016. Wound responses of wild apples suggest multiple resistance mechanism against blue mold decay. Postharvest Biol. Technol. 117, 132–140. https://doi.org/10.1016/j.postharvbio.2015.12.004.

Jimdjio Kouasseu, C., Yang, X., Xue, H., Bi, Y., Liu, Z., Xi, J., Nan, M., Prusky, D., 2023. Reactive oxygen species metabolism modulation on the quality of apple fruits inoculated with *Penicillium expansum* under different ambient pHs. Horticulturae 9, 538. https://doi.org/10.3390/horticulturae9050538.

Kim, D., Paggi, J.M., Park, C., Bennett, C., Salzberg, S.L., 2019. Graph-based genome alignment and genotyping with HISAT2 and HISAT-genotype. Nat. Biotechnol. 37, 907–915. https://doi.org/10.1038/s41587-019-0201-4.

Kim, S.M., Lee, S.M., Seo, J.A., Kim, Y.S., 2018. Changes in volatile compounds emitted by fungal pathogen spoilage of apples during decay. Postharvest Biol. Technol. 146, 51–59. https://doi.org/10.1016/j.postharvbio.2018.08.003.

Köhl, J., Wenneker, M., Groenenboom-de Haas, B.H., Anbergen, R., Goossen-van de Geijn, H.M., Lombaers-van der Plas, C.H., Pinto, F.A.M.F., Kastelein, P., 2018. Dynamics of post-harvest pathogens *Neofabraea* spp. and *Cadophora* spp. in plant residues in Dutch apple and pear orchards. Plant Pathol. 67, 1264–1277. https://doi.org/10.1111/ppa.12854.

Li, C., Cao, S., Wang, K., Lei, C., Ji, N., Xu, F., Jiang, Y., Qiu, L., Zheng, Y., 2021. Heat shock protein HSP24 is involved in the BABA-induced resistance to fungal pathogen in postharvest grapes underlying an NPR1-dependent manner. Front. Plant Sci. 12, 646147 https://doi.org/10.3389/fpls.2021.812672.

Li, H., Ran, K., Dong, Q., Zhao, Q., Shi, S., 2020. Cloning, sequencing, and expression analysis of 32 NAC transcription factors (MdNAC) in apple. PeerJ 2020, e8249. https://doi.org/10.7717/peerj.8249.

Li, M., Leso, M., Buti, M., Bellini, E., Bertoldi, D., Saba, A., Larcher, R., Sanità di Toppi, L., Varotto, C., 2022. Phytochelatin synthase de-regulation in *Marchantia polymorpha* indicates cadmium detoxification as its primary ancestral function in land plants and provides a novel visual bioindicator for detection of this metal. J. Hazard. Mater. 440, 129844 https://doi.org/10.1016/j.jhazmat.2022.129844.

Liao, Y., Smyth, G.K., Shi, W., 2014. featureCounts: an efficient general purpose program for assigning sequence reads to genomic features. Bioinformatics 30, 923–930. https://doi.org/10.1093/bioinformatics/btt656.

Lv, J., Zhang, M., Zhang, J., Ge, Y., Li, C., Meng, K., Li, J., 2018. Effects of methyl jasmonate on expression of genes involved in ethylene biosynthesis and signaling pathway during postharvest ripening of apple fruit. Sci. Hortic. (Amst.). 229, 157–166. https://doi.org/10.1016/j.scienta.2017.11.007.

Maere, S., Heymans, K., Kuiper, M., 2005. BiNGO: a cytoscape plugin to assess overrepresentation of gene ontology categories in biological networks. Bioinformatics 21, 3448–3449. https://doi.org/10.1093/bioinformatics/bti551.

Meng, X., Zhang, S., 2013. MAPK cascades in plant disease resistance signaling. Annu. Rev. Phytopathol. 51, 245–266. https://doi.org/10.1146/annurev-phyto-082712-102314.

Mitchell, A.M., Strobel, G.A., Moore, E., Robison, R., Sears, J., 2010. Volatile antimicrobials from *Muscodor crispans*, a novel endophytic fungus. Microbiology 156, 270–277. https://doi.org/10.1099/mic.0.032540-0.

Negussu, M., Karalija, E., Vergata, C., Buti, M., Subašić, M., Pollastri, S., Loreto, F., Martinelli, F., 2023. Drought tolerance mechanisms in chickpea (*Cicer arietinum* L.) investigated by physiological and transcriptomic analysis. Environ. Exp. Bot. 215, 105488 https://doi.org/10.1016/J.ENVEXPBOT.2023.105488.

Neri, F., Cappellin, L., Aprea, E., Biasioli, F., Gasperi, F., Spadoni, A., Cameldi, I., Folchi, A., Baraldi, E., 2019. Interplay of apple volatile organic compounds with *Neofabraea vagabunda* and other post-harvest pathogens. Plant Pathol. 68, 1508–1524. https://doi.org/10.1111/ppa.13072.

Nybom, H., Ahmadi-Afzadi, M., Rumpunen, K., Tahir, I., 2020. Review of the impact of apple fruit ripening, texture and chemical contents on genetically determined susceptibility to storage rots. Plants 9, 831. https://doi.org/10.3390/plants9070831.

Oh, I.S., Park, A.R., Bae, M.S., Kwon, S.J., Kim, Y.S., Lee, J.E., Kang, N.Y., Lee, S., Cheong, H., Park, O.K., 2005. Secretome analysis reveals an Arabidopsis lipase involved in defense against *Alternaria brassicicola*. Plant Cell 17, 2832–2847. https://doi.org/10.1105/tpc.105.034819.

Park, S.J., Park, S., Kim, Y., Hyeon, D.Y., Park, H., Jeong, J., Jeong, U., Yoon, Y.S., You, D., Kwak, J., Timilsina, R., Hwang, D., Kim, J., Woo, H.R., 2022. Ethylene responsive factor34 mediates stress-induced leaf senescence by regulating salt stress-responsive genes. Plant Cell Environ. 45, 1719–1733. https://doi.org/10.1111/pce.14317.

Pfaffl, M.W., 2001. A new mathematical model for relative quantification in real-time RT–PCR. Nucleic Acids Res. 29, E45 https://doi.org/10.1093/nar/29.9.e45.

Qian, Y., Zhang, T., Yu, Y., Gou, L., Yang, J., Xu, J., Pi, E., 2021. Regulatory mechanisms of bHLH transcription factors in plant adaptive responses to various abiotic stresses. Front. Plant Sci. 12, 677611 https://doi.org/10.3389/fpls.2021.677611.

Ren, C., Kuang, Y., Lin, Y., Guo, Y., Li, H., Fan, P., Li, S., Liang, Z., 2022. Overexpression of grape ABA receptor gene VaPYL4 enhances tolerance to multiple abiotic stresses in Arabidopsis. BMC Plant Biol. 22, 1–14. https://doi.org/10.1186/s12870-022-03663-0.

Robinson, M.D., McCarthy, D.J., Smyth, G.K., 2009. edgeR: a bioconductor package for differential expression analysis of digital gene expression data. Bioinformatics 26, 139–140. https://doi.org/10.1093/bioinformatics/btp616.

Rybakova, D., Müller, H., Olimi, E., Schaefer, A., Cernava, T., Berg, G., 2022. To defend or to attack? Antagonistic interactions between *Serratia plymuthica* and fungal plant pathogens, a species-specific volatile dialogue. Front. Sustain. Food Syst. 6, 1020634 https://doi.org/10.3389/fsufs.2022.1020634.

Scala, A., Mirabella, R., Mugo, C., Matsui, K., Haring, M.A., Schuurink, R.C., 2013. E-2-hexenal promotes susceptibility to *Pseudomonas syringae* by activating jasmonic acid pathways in Arabidopsis. Front. Plant Sci. 4, 42974. https://doi.org/10.3389/fpls.2013.00074.

Shen, G., Sun, W., Chen, Z., Shi, L., Hong, J., Shi, J., 2022. Plant GDSL esterases/lipases: evolutionary, physiological and molecular functions in plant development. Plants 11, 468. https://doi.org/10.3390/plants11040468.

Smith, R.B., Lougheed, E.C., Franklin, E.W., McMillan, I., 1979. The starch iodine test for determining stage of maturation in apples. Can. J. Plant Sci. 59, 725–735. https://doi.org/10.4141/cjps79-113.

Son, G.H., Wan, J., Kim, H.J., Nguyen, X.C., Chung, W.S., Hong, J.C., Stacey, G., 2012. Ethylene-responsive element-binding factor 5, ERF5, is involved in chitin-induced innate immunity response. Mol. Plant-Microbe Interact. 25, 48–60. https://doi.org/10.1094/MPMI-06-11-0165.

Strobel, G.A., Dirkse, E., Sears, J., Markworth, C., 2001. Volatile antimicrobials from *Muscodor albus*, a novel endophytic fungus. Microbiology 147, 2943–2950. https://doi.org/10.1099/00221287-147-11-2943.

Ul Haq, S., Khan, A., Ali, M., Khattak, A.M., Gai, W.X., Zhang, H.X., Wei, A.M., Gong, Z. H., 2019. Heat shock proteins: Dynamic biomolecules to counter plant biotic and abiotic stresses. Int. J. Mol. Sci. 20, 5321. https://doi.org/10.3390/ijms20215321.

Wickham, H., 2016. ggplot2 elegant graphics for data analysis. Use R! Ser. 211.

Xu, Y., Tong, Z., Zhang, Xiaochen, Zhang, Xing, Luo, Z., Shao, W., Li, L., Ma, Q., Zheng, X., Fang, W., 2021. Plant volatile organic compound (*E*)-2-hexenal facilitates

Botrytis cinerea infection of fruits by inducing sulfate assimilation. N. Phytol. 231, 432–446. https://doi.org/10.1111/nph.17378.

Žebeljan, A., Vico, I., Duduk, N., Žiberna, B., Urbanek Krajnc, A., 2019. Dynamic changes in common metabolites and antioxidants during *Penicillium expansum*-apple fruit interactions. Physiol. Mol. Plant Pathol. 106, 166–174. https://doi.org/10.1016/j.pmpp.2019.02.001.

Zhang, J., Li, Y., Du, S., Deng, Z., Liang, Q., Song, G., Wang, H., Yan, M., Wang, X., 2023. Transcriptomic and proteomic analysis reveals (*E*)-2-hexenal modulates tomato resistance against *Botrytis cinerea* by regulating plant defense mechanism. Plant Mol. Biol. 111, 505–522. https://doi.org/10.1007/s11103-023-01339-3.